RSC Advances

ROYAL SOCIETY OF CHEMISTRY

www.rsc.org/advances

Persistent luminescent and photocatalytic properties of $Zn_xGa_2O_{3+x}$ ($0.8 \leq x \leq 1$) phosphors

Darong Li, Yinhai Wang*, Ke Xu, Hui Zhao, Zhengfa Hu

(School of Physics and Optoelectronic Engineering, Guangdong University of Technology, Waihuan Xi Road, No.100, Guangzhou 510006, People's Republic of China)

([*]Corresponding author. Fax: +86-20-39322265, E-mail: yhwang@gdut.edu.cn)

Abstract

The $Zn_xGa_2O_{3+x}$ (x=1, 0.95, 0.9, 0.85, 0.8) phosphors were synthesised successfully via high temperature solid-state reaction. The photoluminescent, persistent luminescent and photocatalytic properties of the phosphors had been studied systematically. The results indicated that their excitation and emission spectra were similar to that of $ZnGa_2O_4$ phosphors and all of them have excellent persistent luminescent and photocatalytic properties. The optical properties were changed with the ratio of the Zn^{2+}/Ga^{3+} and the $Zn_{0.85}Ga_2O_{3.85}$ phosphor shown the best persistent luminescent and photocatalytic properties. The $Zn_{0.85}Ga_2O_{3.85}$ phosphor can be effectively activated by an ultraviolet lamp and ultraviolet excitation can lead to 10 min of persistent green emission. Moreover, the $Zn_{0.85}Ga_2O_{3.85}$ could provide more defect energy levels which can act as photogenerated electron traps and maintain the electron-hole pairs for a longer period, enhancing the persistent luminescent and photocatalytic performance.

Keywords: Phosphors; Persistent luminescence; Photocatalytic; Trap

1. Introduction

Persistent luminescence is an optical phenomenon, whereby a material is excited with radiation and resulting in luminescent emission remains visible for a long time (seconds to many hours) after the excitation has stopped [1-3]. These materials are drawing more and more attention in recent years due to the great potential applications in many field, such as emergency signage, traffic signs and vivo bio-imaging.

Recently, zinc gallate ($ZnGa_2O_4$) phosphor has attracted much attention for use in field emission display (FED) and thin film electroluminescence device (TFED), because $ZnGa_2O_4$ phosphor shows higher chemical and thermal stability than sulfide phosphors [1, 2]. $ZnGa_2O_4$ crystallizes in the normal spinel structure (Fd3m) with Ga^{3+} ions occupying octahedral sites and Zn^{2+} ions occupying tetrahedral sites. Its band gap is about 4.4 eV, and it exhibits a strong blue emission for material not doped with impurities [2]. $ZnGa_2O_4$ can also act as a host material for multicolor emitting phosphor when doped with transition metals: Cr-doped $ZnGa_2O_4$ ($ZnGa_2O_4:Cr^{3+}$) for red emission [3] and Co-doped $ZnGa_2O_4$ ($ZnGa_2O_4:Co^{3+}$) for reddish orange emission [4]. In addition, $ZnGa_2O_4$ has excellent performance in air-pollution control. Because $ZnGa_2O_4$ has hybridized orbitals of Zn4s4p, Ga4s4p and the wide band gap (4.4 eV), it can improve the mobility of photogenerated electrons and the absorption efficiency in ultraviolet (UV) lamps [5]. Some papers reported that high temperature reaction triggered the vaporization of zinc ions and formed intrinsic defect in the hosts [4, 5]. Thus, $ZnGa_2O_4$ exhibits the persistent luminescent characteristics. However, the influence of zinc deficiency on the persistent luminescent and photocatalytic performance of $ZnGa_2O_4$ phosphor is rarely reported.

In this study, we synthesised the $ZnGa_2O_4$ phosphor with slightly Zn-deficient composition successfully and investigated their effects on the luminescent, persistent luminescent and photocatalytic properties. The mechanism for enhancement of persistent luminescent and photocatalytic properties was also discussed.

2. Experimental

The $ZnGa_2O_4$ phosphors were synthesised via high temperature solid-state reaction method. ZnO powder (99.9%), Ga_2O_3 powder (99.9%) were milled for about 30 min in an agate mortar. The stoichiometric proportions of raw materials were weighed according to the nominal compositions of $ZnGa_2O_4$ (S_1), $Zn_{0.95}Ga_2O_{3.95}$ (S_2), $Zn_{0.9}Ga_2O_{3.9}$ (S_3), $Zn_{0.85}Ga_2O_{3.85}$ (S_4), $Zn_{0.8}Ga_2O_{3.8}$ (S_5), respectively. Then the mixtures were moved into a corundum crucible and sintered at 1300 ℃ for 5 hours in an air ambient.

The X-ray powder diffraction (XRD) verified the phase structure of all samples by using a diffractometer with Cu Kα irradiation (λ=1.5406 Å) at 36 KV tube voltage and 20 mA tube current. We set the scanning range from 10° to 70°. The excitation, emission spectra and afterglow decay were measured by a Hitachi F-7000 Florescence Spectrophotometer. Prior to the afterglow decay measurements, the samples were excited by an UV lamp (λ_{ex}=254 nm) for 5 min. Then measurement was in a dark place without excitation. The thermoluminescent (TL) curves were recorded by a FJ427A1 thermoluminescent dosimeter. The heating rate was 1℃/s for all samples. Prior to the TL measurement, each sample was first exposed to an UV lamp (λex=254 nm) for 2 min and then put in dark waiting for 3 min.

The photocatalytic degradation tests were carried out in photoreactor (BL-GHX-V), using 50mg S_1, S_2, S_3, S_4 and S_5 powder dispersed in 200ml Rhodamine B (RhB) aqueous solution (10 mg/L), respectively.

The mixture aqueous solution was put into a beaker with magnetic stirring for 30 min. The light source was a 500 W UV lamp and continuous magnetic stirring should be maintained the suspension of powder in the RhB solution. Then 5 mL of the suspension was gathered for every 10 min and measured via an Ultraviolet-visible Light Spectrometer by measuring its absorbance at a wavelength of 550 nm.

3. Results and discussion

The XRD patterns of five samples are shown in Fig. 1. The diffraction peaks of S_1 can be indexed as a pure cubic spinel (space group Fd3m) phase $ZnGa_2O_4$, and all diffraction peaks are in good agreement with the standard data of $ZnGa_2O_4$. For S_4 and S_5, extra peaks are appeared in addition to the peaks of $ZnGa_2O_4$, which correspond to the phase of β-Ga_2O_3. It reveals that the obtained products are the mixture of $ZnGa_2O_4$, β-Ga_2O_3 and $Zn_xGa_2O_{3+x}$. Compared with the standard data of JCPDS no. 38-1240, there is no apparent shift can be found in all samples.

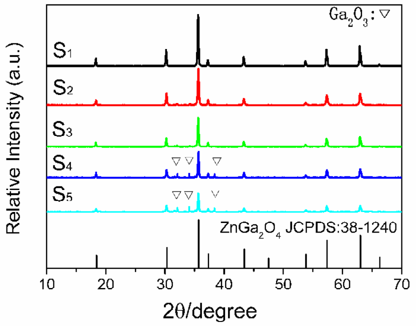

As a kind of self-activated phosphor, $ZnGa_2O_4$ emits blue emission. Fig. 2a shows the excitation and emission spectra of $Zn_xGa_2O_{3+x}$ (x=1, 0.95, 0.9, 0.85, 0.8) phosphors. The excitation spectrum monitored at 430 nm shows a broad band from 230 nm to 280 nm with the peak position at 254 nm, which can be attributed to the charge transfer of Ga-O [2]. Under excitation with 254 nm UV, the emission spectrum of all samples consists of a broad band ranging from 390 nm to 520 nm with a maximum at 430 nm, which is originated from the self-activation center of the octahedral Ga-O group in the $ZnGa_2O_4$ lattices [2, 5]. Moreover, there is a weak emission peak at 500 nm which can be attributed to the $^2E_A \rightarrow ^4A_2$ transition of Ga^{3+} in the distorted octahedral [2, 5]. The red shift phenomenon in the emission with the decrease of Zn^{2+} concentration is observed. Because the ionic radii of the Ga^{3+} is greater than Zn^{2+}, the radii of the ions are as follows: $R(Zn^{2+})=0.060$nm, $R(Ga^{3+})=0.062$nm [6]. The Zn^{2+} substituted by the Ga^{3+} increases the lattice constant of $ZnGa_2O_4$. Thus, the peak of emission shifts toward long wavelength. The decay curves of five samples recorded within 0–600 s are presented in Fig. 2b. As can be seen, all samples exhibit similar decay processes which contain a rapid decay at beginning and a slow decay process afterward [7, 8]. The sequence of the initial intensity for different Zn^{2+} concentration is $x=0.85>x=0.9>x=0.8>x=0.95>x=1.0$. In our study, the decay curves can be well fitted by a double-exponential equation and as follows:

$$I = I_1\, exp(\frac{-t}{\tau_1}) + I_2\, exp(\frac{-t}{\tau_2})$$

where $I(t)$ is phosphorescence intensity; I_1 and I_2 are constants which represent the rapid and slow initial luminescent intensity at t=0 s; τ_1 and τ_2 are the decay constants, which decide rapid decay and slow decay components, respectively, and the decay duration depends on the second exponential [9]. According to the above formulas, the fitting results are listed in Fig. 2c. These parameters indicate that $Zn_{0.85}Ga_2O_{3.85}$ is the optimal value to produce the persistent luminescence, and the duration is about 10 min (>0.35 mcd/m^2). The persistent luminescence of five samples is visually evaluated using a fluorescence microscopy in the dark environment. The inset of Fig. 2b shows the changes of emission “brightness” with a decay time up to 10 min after exposure to an UV lamp (λ_{ex}=254 nm) for 5 min. It clearly shows that S_4 can be effectively activated by an UV lamp and UV excitation can lead to 10 min persistent green emission.

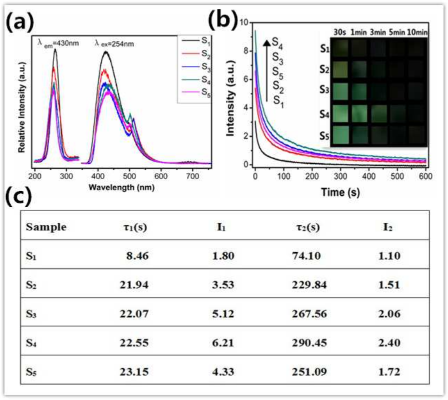

Sample	τ_1(s)	I_1	τ_2(s)	I_2
S_1	8.46	1.80	74.10	1.10
S_2	21.94	3.53	229.84	1.51
S_3	22.07	5.12	267.56	2.06
S_4	22.55	6.21	290.45	2.40
S_5	23.15	4.33	251.09	1.72

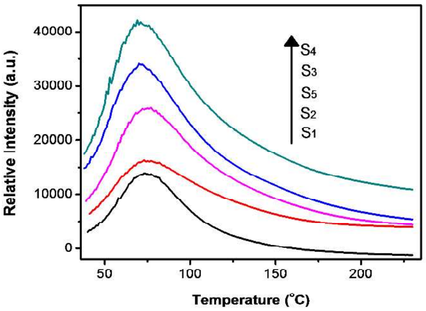

As already known**,** thermoluminescence (TL) measurement provides an efficient way to reveal the information of traps. In general, the trap concentration is approximately proportional to the TL intensity and the maximum temperature of the TL peak provides information on the depth of the carrier trap [9-11], and the optimal TL peak is usually located at the temperature range of 50-120℃ for the excellent persistent luminescent properties [9, 11]. As shown in Fig. 3, S_1 shows a quite weak TL band centered at 75℃ which confirms the poor persistent luminescence. The TL curves of S_2, S_3, S_4 and S_5 have the same peak location and similar shape to that of S_1, but their intensity are largely enhanced, and it indicates a higher defect concentration. It is well known that the ZnO is volatilized during $ZnGa_2O_4$ synthesis due to the high vapor pressure. One vacancy defect of V_o^{++} with 2 positive charges and one vacancy defect of V_{Zn}** with 2 negative charges would be created in the host. Then the Ga^{3+} ions would occupy the defect of V_{Zn}^{**} and from Ga_{Zn}^{+}, which act as the electron trap. And the defect of V_o^{++} would transform into the V_o^{*} and act as the hole trap. Moreover, more Ga^{3+} ions occupy the V_{Zn}^{**} sites with Zn^{2+} deficient, which will raise the concentration of the Ga_{Zn}^{+} (electron trap). Therefore, the persistent luminescence enhances firstly. However, the distance of Ga-Ga would be shortened as the concentration of Ga_{Zn}^{+} continues to raise with Zn^{2+} deficient, the concentration quenching occurs. Thus, the persistent luminescence begins to decrease.

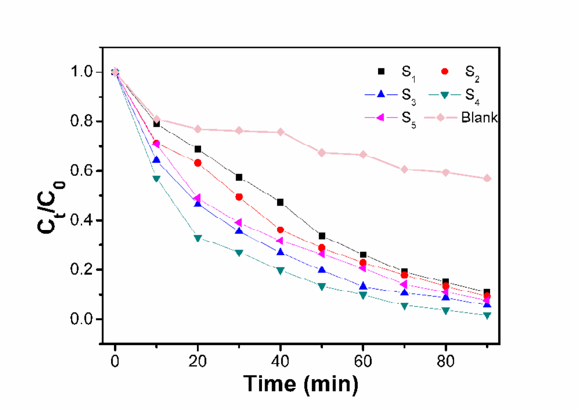

Fig. 4 shows photocatalytic activity as a function of irradiation time with different Zn^{2+} ion concentration. It can be seen that with the decrease of Zn^{2+} concentration, the photocatalytic activities of $Zn_xGa_2O_{3+x}$ (x=1, 0.95, 0.9, 0.85, 0.8) first increase and then decrease. The $Zn_{0.85}Ga_2O_{3.85}$ phosphor exhibits the highest photocatalytic activity, and the decomposition rate for the S_4/Rhodamine B (RhB) composites reached 98.5% after 90 min. As we known, the high density of surface hydroxyls, proper band positions, broad hybridized orbitals, and large surface area all would improve the high photocatalytic activity of $ZnGa_2O_4$ [12]. And $ZnGa_2O_4$ could provide more defect energy levels which can act as photogenerated electrons trap and maintain the electron-hole pairs for a while, enhancing the photocatalytic performance [13, 14]. In our case, a large numbers of oxygen vacancies have been found in $ZnGa_2O_4$ phosphors as evident from TL results. The oxygen vacancies act as an electron traps, which implies a decreased recombination rate of the electrons and holes. The large numbers of oxygen vacancies generate more hydroxyl radicals on the surface, and the strong redox ability of photogenerated electron-hole pairs may also improve the photocatalytic performance. The UV-Vis diffuse reflectance spectra of $Zn_xGa_2O_{3+x}$ are displayed in Fig. 5(a). And the band gap is determined based on the UV-Vis spectra and is displayed in Fig. 5(b). It can be seen that with Zn^{2+} ion concentration decreases, E_g (band gap energy) of $Zn_xGa_2O_{3+x}$ decreases, increasing higher UV utility efficiency. Thus, photocatalytic activity is improved. However, the reducing of E_g would make E_{VB} (valence bands) and E_{CB} (conduction band) of $Zn_xGa_2O_{3+x}$ phosphors shift to the Fermi level and decrease the redox ability of photogenerated electron-hole pairs [15, 16]. Thus, further decrease of Zn^{2+} concentration may lead to decrease in photocatalytic performance of $ZnGa_2O_4$.

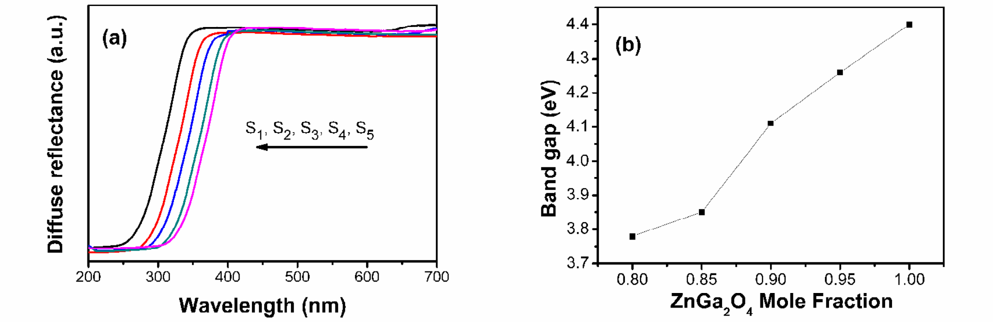

4. Conclusion

In summary, the $Zn_xGa_2O_{3+x}$ (x=1, 0.95, 0.9, 0.85, 0.8) phosphors were synthesised via high temperature solid-state reaction successfully. The influence of Zn^{2+} ions concentration on PL, decay curves, TL and photocatalytic activity were studied in detail. The emission intensity decreases and the peak of emission shifts toward long wavelength with the decrease of Zn^{2+} ion concentration. The $Zn_{0.85}Ga_2O_{3.85}$ phosphor can be effectively activated by an UV lamp and the UV excitation can lead to 10 min of persistent green emission. According to the analysis of TL curves, it can be supposed that more Ga^{3+} ions occupy the V_{Zn}^{**} sites with Zn^{2+} deficient, which will raise the concentration of electron trap. However, the distance of Ga-Ga would be shortened as the concentration of Ga_{Zn}^{+} continues to raise, the concentration quenching occurs. Studies of the $ZnGa_2O_4$ phosphor photocatalytic activity have indicated that with Zn^{2+} ion concentration decreases, E_g (band gap energy) of $Zn_xGa_2O_{3+x}$ decreases, increasing higher UV utility efficiency. And photocatalytic activity is improved. But the reducing of E_g would make E_{VB} and E_{CB} of $Zn_xGa_2O_{3+x}$ phosphors shift to the Fermi level and decrease the redox ability of photogenerated electron-hole pairs. Therefore, photocatalytic performance first increases and then decreases at the same condition.

Acknowledgments

This work is supported by the National Nature Science Foundation of China (No.21271048) and State Key Laboratory of Rare Earth Resource Utilization Open Projects (RERU2013007).

References

1. M. Allix, S. Chenu, E. Véron, T. Poumeyrol, E.A. Kouadri-Boudjelthia, S. Alahraché, F. Porcher, D. Massiot and F. Fayon, Chem Mater., 2013, 25, 1600.

2. W.N. Kim, H.L. Park and G.C. Kim, Mater Lett., 2005, 59, 2433.

3. Y. Zhuang, J. Ueda and S. Tanabe, Appl Phys Express., 2013, 6, 052602.

4. L.P. Sosmana, T. Abrittaa, A.C. Pereirab and H. Vargasb, Chem Phys Lett., 1994, 227, 485.

5. W. Zhang, J. Zhang, X. Lan, Z. Chen and T. Wang, Catal Commun., 2010, 11, 1104.

6. R.D. Shannon, Acta. Cryst., 1976, 32, 751.

7. P. Huang, D. Liu, C.E. Cui, L. Wang and G. Jiang, Appl. Phys. A., 2014, 116, 759.

8. Y. Zhuang, J. Ueda and S. Tanabe. J Mater Chem C., 2013, 1, 7849.

9. Y. Jin, Y. Hu, L. Chen, X. Wang, Z. Mu, G. Ju and T. Wang. Mater Lett., 2014, 126, 75.

10. X. Xu, X. Zhang, T. Wang, J. Qiu and X. Yu. Mater Lett., 2014, 127, 40.

11. W. Xie, Y. Wang, C. Zou, J. Quan and L. Shao. J. Alloys Compd., 2015, 619, 244.

12. H. Li, S. Yin, Y. Wang, T. Sekino, S.W. Lee and T. Sato. J Mater Chem A., 2013, 1, 1123.

13. W.S. Tung, W.A. Daoud and G. Henrion. Thin Solid Films., 2013, 545, 310.

14. X. Wang, M. Blackford, K. Prince and R. A. Caruso. Appl Mater Interfaces., 2012, 4, 476.

15. Y. An, L. Yang, J. Hou, Z. Liu and B. Peng. Opt. Mater., 2014, 36, 1390.

16. H. Li, S. Yin and T. Sato. Appl. Catal. B., 2011, 106, 586.

Figure captions

Fig.1 XRD patterns of all samples.

Fig.2 (a) Excitation and emission spectra of all samples; (b) persistent luminescent decay curve after irradiation by 254 nm and images of all samples taken at different persistent luminescence times; (c) the fitting results of decay curves. The phosphors were irradiated for 5 min.

Fig.3 TL curves of all samples.

Fig.4 Degradation of RhB in the presence of all samples. The light source was a 500 W UV lamp.

Fig.5 (a) The UV-Vis diffuse reflectance spectra; (b) optical band gap E_g of all samples.